A COMPARISON OF ACOUSTIC SOLVERS FOR FT ULTRASONIC WIND SENSORS

Antonio Jimenez-Garcia[1*]
Ganesh Chandrasen Diwan[2]

[1]Lead Research Engineer, FT Technologies, Sunbury House, Sunbury-on-Thames, TW16 7DX, UK
[2]Acoustic Researcher, Prescient Computing, Woking, GU21 3HT, UK

ABSTRACT

FT wind sensors measure wind speed and direction by using an acoustic field that is superimposed on a flow field in an acoustic resonator equipped with piezoelectric transducers. To improve the accuracy of wind measurements in compliance with the evolving requirements of the wind energy industry, the geometric design of FT wind sensors went through several design iterations to optimise the acoustic field and its interaction with the flow field. Finite Element based simulation tools are used to research and rapidly optimise the acoustic behaviour of FT wind sensors. The Multiphysics Research team ensures that the accuracy and reliability of the numerical methods and simulation software are adequate.

In this paper, two acoustics software packages are compared, namely COMSOL Multiphysics®, a commercial software and NGSolve, an open-source general-purpose finite element library. First, a mesh convergence study is presented using a canonical 3D acoustic scattering problem. A practical application of FT wind sensors is then studied to assess the accuracy of both software. In this regard, the effect of different boundary treatments such as impedance condition and Perfectly Matched Layer are evaluated. Finally, CPU overhead of the direct solvers is also presented.

***Keywords*—**acoustic solvers, comsol, ngsolve, finite element method, acoustic resonance

1. INTRODUCTION

FT Technologies [1] follows an iterative research prototyping in the design of its wind sensor geometries. The methodology involves the design, testing, and evaluation of prototypes, taking into account a multiphysics perspective that specifically emphasizes acoustics, aerodynamics, and aeroacoustics amid other relevant disciplines. The capability to numerically simulate the physics of the interaction of acoustic and aerodynamic fields and the geometry enables us to improve our current designs and iterate over future sensor designs.
Consequently, FT Technologies relies on high-fidelity numerical models and on the accuracy of numerical methods to address the complexity of sensor acoustics and aerodynamics [2] within the realm of ultrasonic frequencies, turbulent flow, and high velocities. The analytical solutions for acoustic fields for such complex geometries are almost impossible to build and a combination of numerical simulations and experimental data is therefore required. Frequently, numerical simulations provide a deeper understanding of the underlying physics of the problem, revealing insights that may remain inaccessible through experimental measurements alone. It is crucial, however, when using numerical techniques to guarantee the high accuracy of the numerical methods through the use of appropriate boundary conditions, quality of the mesh, convergence of the solution, and numerical stability [3].

In this context, this paper aims to conduct a comparison between two acoustic software to accurately resolve in the absence of flow, the acoustic field of FT wind sensors governed by the scalar Helmholtz equation. The commercial software COMSOL Multiphysics® [4] and NGSolve [5], an open-source finite element library are utilized here. The analytical solution of the scattering of waves from a spherical obstacle [6] with a diameter matching that of an FT wind sensor is first numerically studied to showcase the convergence of both software as the frequency increases from 20 kHz to 40 kHz. The sensitivity of the solution to changes in the mesh density and the use of first-order and second-order Lagrange discretization schemes are evaluated. Next, a simplified geometry of an FT wind sensor is employed to investigate how the size of the computational domain and the density of the mesh impact the acoustic field with the use of both software. Subsequently, the effectiveness of reducing reflections at the computational domain's boundaries is explored using the Perfectly Matched Layer (PML) and Acoustics Impedance techniques. Finally, the CPU load is documented, and conclusions are drawn based on the numerical outcomes, resulting in the formulation of recommendations.

2. ACOUSTIC SIMULATION SOFTWARE

In this study, two acoustic simulation software are numerically compared for the purpose of resolving acoustic fields. The following paragraph provides a concise introduction to both software tools.

2.1. COMSOL Multiphysics® Software

The COMSOL Multiphysics® software [4] is a powerful commercial simulation software package that addresses the numerical modelling

* ***Corresponding author**: antonio.jimenez-garcia@fttechnologies.com*

of singe-physics and coupled multiple disciplines such as electromagnetics, fluid flow, heat transfer, chemical reactions, structural mechanics, and acoustics. It offers a streamlined workflow that encompasses the entire process of modelling, starting from geometry generation to the analysis of results. Multiple numerical methods are available for modelling pressure acoustics, including the following: Finite Element Method (FEM), Boundary Element Method (BEM), and Hybrid FEM-BEM in the frequency domain and the discontinuous Galerkin finite element method (dG-FEM) in the time domain [7]. For efficiently addressing radiation and scattering problems with complex geometries, the FEM proves to be a suitable approach for smaller-scale problems. Consequently, in this research, the FEM is employed along with either the PMLs or impedance boundary conditions to simulate the behaviour of the unbounded computational domain.

All the modelling steps such as defining the physics, boundary conditions, discretization order and solver settings are defined through a single graphical user interface. The meshing is performed by COMSOL Multiphysics® using its own meshing algorithm and it can handle three-dimensional geometries and various element types, including tetrahedral, hexahedral, pyramidal, and prismatic. To solve the systems of linear equations, direct and iterative solvers are available in COMSOL Multiphysics®. For problems characterized by a small number of degrees of freedom and lower memory demands, selecting a direct solver such as MUMPS often proves to be the more advantageous choice [7]. For large 3D models, the first suggestion is to use iterative methods such as the multigrid, including GMRES with GMG and FGMRES with GMG for problems that exhibit sharp resonances [7].

2.1. NGSolve Software

NGSolve [5] is an open-source finite element library built on top of Netgen/NGSolve and enables the implementation of physical equations and algorithms through a user-friendly Python interface. It also offers a unified analysis framework that is available via a GUI by providing a seamless integration of all the steps from geometrical modelling to analysis and visualization. Similar to the preceding section featuring COMSOL Multiphysics®, the FEM is utilized in the context of NGSolve. Within the framework of FEM, the choice of test functions and basis functions lead to different finite element method formulations. The Galerkin method is used to discretize the mathematical model equations for both software.

The three-dimensional finite element mesh generator Gmsh [8] is employed and it has been integrated into NGSolve's framework. It can also handle various types of two and three-dimensional elements. Both direct and iterative solvers are available within NGSOLVE. To facilitate comparison in terms of CPU loads with COMSOL Multiphysics®, a direct solver has been chosen as the primary option.

3. GOVERNING EQUATION

The analysis of the scattering of waves from a spherical obstacle alongside the acoustic field of FT wind sensors in the absence of flow is governed by the scalar Helmholtz equation. For an inviscid, compressible, and irrotational fluid, with no mean flow or source term, the acoustic pressure, p satisfies the wave equation (1), see [9].

$$\nabla^2 p - \frac{1}{c^2}\frac{\partial^2 p}{\partial t^2} = 0 \tag{1}$$

with c being the speed of sound. For a time-harmonic vibration at pulsation ω with amplitude P, such that $p = Pe^{i\omega t}$, the equation (1) reduces to the scalar Helmholtz equation (2):

$$\nabla^2 p + k^2 p = 0 \tag{2}$$

Here $k = \omega/c$ represents the wavenumber, which is also equivalent to $k = 2\pi/\lambda$ with λ being the wavelength of the acoustics pressure. In this study, the following boundary conditions are considered.

Sound-hard boundary (wall): The normal component of the velocity is zero. In simple terms, this also refers to the normal derivate of the total acoustic pressure being zero, thus, $\partial p/\partial \mathbf{n} = 0$ where $\mathbf{n}$ is the unit normal vector to the wall.

Prescribed normal velocity: It relates the velocity to acoustic pressure as $v_{\mathrm{n}} = -i\frac{1}{\rho\omega}\partial p/\partial \mathbf{n}$, where ρ is the density of the medium and i the imaginary unit.

Sommerfeld radiation condition: For an exterior problem, the acoustic wave radiates from a source must scatter to infinity and this is mathematically expressed as the Sommerfeld radiation condition [10]:

$$\lim_{|\mathbf{r}|\to\infty} |\mathbf{r}| \left(\frac{\partial}{\partial|\mathbf{r}|} + \mathrm{i}k\right) p(\mathbf{r}) = 0 \tag{3}$$

here $\mathbf{r}$ denotes the position vector of a point in three-dimensional space with respect to origin. The system of equations (2)-(3) with boundary conditions forms the Helmholtz equation system that needs to be solved with an appropriate numerical method.

The absorption of sound in air through thermal conduction effects, viscous effects, and molecular relaxation [11] processes are not accounted for in this study. In this context, pressure acoustics is only modelled.

4. PROBLEM FORMULATION AND NUMERICAL STUDIES

In this section, numerical outcomes corresponding to the scattering of plane wave by a rigid sphere, as well as the acoustic field of a simplified geometry of the FT wind sensor are showcased through the use of the NGSolve and COMSOL Multiphysics® software.

The acoustics resonance anemometer, invented by Savvas Kapartis [12], measures phase shifts between a pair of transducers induced by the flow of a fluid within an acoustic resonant cavity. A standing wave perpendicular to the direction of the flow of the fluid and a travelling wave perpendicular to the standing wave is created in the acoustic resonant cavity and it is energised by one of the three ultrasonic transducers. Through the utilization of phase shifts at resonance between the acoustic signal of a pair of transducers, it is possible to compute the fluid flow velocity and its direction. The sensor inherently compensates for variations in the environment, specifically, temperature, humidity and pressure, resulting in a technology immune to changes in the speed of sound. Furthermore, operating within ultrasonic resonances offers a high signal-to-noise ratio advantage. This, in combination with a solid-state (no moving parts) technology, provides a well-suited anemometer for a diverse harsh environmental scenario where accuracy both on the flow field and direction is essential.

Figure 1 shows a simplified FT742 wind sensor geometry where grooves, notches, and turbulators were removed and the resonator cavity was simplified. The sensor has an external diameter of 55 mm and the entrance to the resonator cavity measures 9.5 mm. This in combination with an internal step of 0.5 mm results in a resonator gap of 10 mm.

The structural mechanical and piezoelectricity coupling of the transducers with the acoustic resonator anemometer is not modelled in this study. Instead, the transducers are modelled using a prescribed normal velocity.

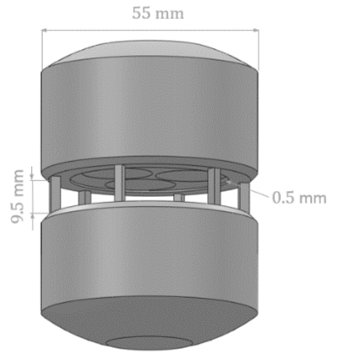

Figure 1: Simplified FT742 wind sensor geometry [1].

As stated earlier, FT wind sensors operate within the ultrasonic frequency range and in the absence of flow, the standing wave generated inside the acoustic resonator is excited a one wavelength, coinciding with the resonator gap of 10 mm. At an ambient temperature of 20°C and with zero wind speed, the resonance frequency is determined to be 35.2 kHz.

4.1 Scattering of Plane Wave from a Spherical Obstacle

The analysis of the scattering of waves from a rigid spherical obstacle is a well-studied problem in acoustics [6]. It contains an analytical solution that can serve as a reference for assessing the performance of acoustics software. In this context, this canonical problem is employed to illustrate the convergence of the numerical methods, as accurately capturing scattering becomes more challenging with increasing frequency [13].

Let us assume that a plane wave of the form $p_p e^{ikx}$ is propagating in the x-direction and is impinged upon a rigid sphere of radius a. The analytical solution for the scattered pressure field due to the incident plane wave is given by [14]:

$$p_s(r,\theta) = -p_p \sum_{m=0}^{\infty} (2m+1) i^m \frac{J_m'(ka)}{H_m'(ka)} P_m(\cos\theta) H_m(kr) \quad (4)$$

where J_m is the spherical Bessel function of the first kind, $H_m$is the spherical Hankel function of the second kind, P_m is the Legendre function of the first kind, and (r,θ) are the polar coordinates. The primed function such as $J_m'(ka)$ indicates a derivative of $J_m(ka)$ with respect to its argument ka. The total pressure is computed as the sum of the incident field and scattered field, with $p_p = 1$ and is given by:

$$p = p_s + p_p e^{ikx} \quad (5)$$

NGSolve and COMSOL Multiphysics® acoustics software are employed to calculate the numerical error, denoted here as p_h, with respect to the analytical solution p. A direct solver is used for both software. The error in the finite element solution p_h is given by the following equation:

$$e_h = \frac{\|p - p_h\|_{\Omega_h}}{\|p\|_{\Omega_h}}$$

where Ω_h is the domain of computation discretized using a finite element mesh. Given the three-dimensional nature of the FT wind sensor, it is advisable to assess the performance of both acoustic solvers using a spherical scattering problem. To align with the 55 mm diameter of the sensor (see Figure 1), it is adopted here a sphere with a diameter of 55 mm for this study. The medium considered here is air with a speed of sound equal to 343.2 m/s.

The spherical symmetry of the problem is exploited here to simulate just one-quarter of the complete geometry. The sensitivity of the numerical solution to changes in the mesh density and the use of first-order (linear elements) and second-order (quadratic elements) Lagrange discretization schemes is evaluated. The analysis is taken within ultrasonic frequency range, specifically at the frequencies of 20 kHz, 35.2 kHz, and 40 kHz. Table 1 lists the numerical cases performed with the solvers NGSolve and COMSOL Multiphysics®. Number of elements per wavelength elm/λ equal to 4, 8, 10, 12, and 16 are evaluated with a first-order Lagrange, while 4, 8, and 10 are considered with a second-order.

Table 1: Numerical cases performed with NGSolve and COMSOL Multiphysics®, illustrating the discretization order and number of elements per wavelength employed.

Discretization Order	elm/λ
First-order Lagrange (p1)	4, 8, 10,12, 16
Second-order Lagrange (p2)	4, 8, 10

Figure 2 shows a comparison between the two software in calculating the L^2 −errors using first-order Lagrange elements at frequencies of 20 kHz, 35.2 kHz, and 40 kHz. As the mesh undergoes refinement levels by increasing the number of elements per wavelength, a gradual reduction is observed in the relative L^2 −error, e_h with both software. Nonetheless, a minimum of 12 elements per wavelength is necessary to achieve a reduction in the L^2 −errors below 10%.

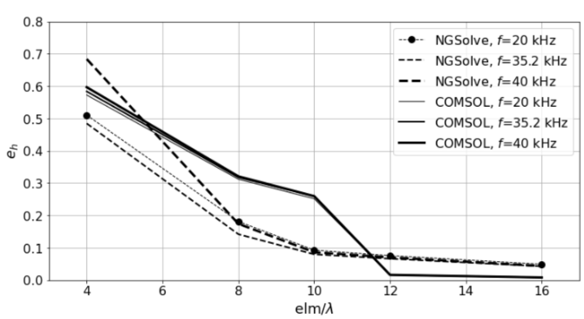

Figure 2: Comparison between NGSolve and COMSOL® for the scattering of a plane wave from spherical obstacle of diameter 55 mm, illustrating L^2 −errors for frequencies of 20 kHz, 35.2 kHz and 40 kHz using first-order Lagrange elements.

Reducing the number of elements per wavelength can be achieved by increasing the order of the discretization elements. In this regard, Figure 3 shows the relative L^2 −error using a second-order Lagrange approximation. In order to reduce the L^2 −errors within (10^{-1}) for this canonical problem, the use of at least 8 elements per wavelength with second-order Lagrange approximation would be required.

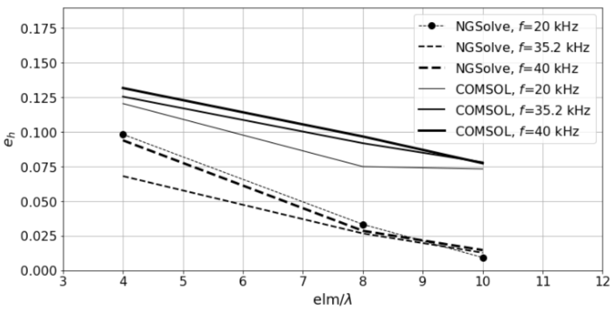

Figure 3: Comparison between NGSolve and COMSOL® for the scattering of a plane wave from spherical obstacle of diameter 55 mm, illustrating L^2 −errors for frequencies of 20 kHz, 35.2 kHz and 40 kHz using second-order Lagrange elements.

4.2 Simplified Geometry of FT Wind Sensor

The acoustic field of a simplified geometry of an FT wind sensor (depicted in Figure 1) is investigated using the NGSolve and COMSOL Multiphysics® software. Transducers are not explicitly modelled; instead, a unit normal velocity is applied to the transmitting transducer. In each case, the total acoustic pressure response is first averaged over the surface of the receiving transducer and then normalized by its maximum value. Quadratic Lagrange was selected for all computations and a frequency sweep from 34.6 kHz to 36 kHz with 20 Hz step was chosen. Computations were performed on a Desktop PC with Intel(R) Core(TM) i9-10900K CPU at 3.70 GHz clock speed, 64 Gb of memory.

4.2.1. Results of COMSOL Multiphysics® Acoustic Software

The impact of changes in mesh density on the acoustic field of the simplified geometry is initially studied using an identical computational domain. The simulation covers the entire domain, including the three transducers and number of elements per wavelength of 4, 6, and 8. The horizontal distance to the PML boundaries remains constant and is set to 3 λ. The computational details of this initial test group (effect of the mesh density) are listed in Table 2 and indicated as ID01, ID02, and ID03. Figure 4 (a) illustrates the dimensions of the extended computational domain alongside the boundary conditions employed, utilizing a symmetry plane to enhance clarity. Details of the surface and volume mesh using a PML boundary condition using the coarsest (4 elm/λ) and finest (8 elm/λ) meshes are illustrated in Figure 5. The primary body consists of tetrahedral elements while the PML region employs hexahedral elements. A consistent six elements per wavelength is kept constant within that region and in line with recommended practice in COMSOL Multiphysics®.

The acoustic response as a function of the mesh density is shown in Figure 6. The first peak observed at 35,200 Hz aligns with the resonator's second harmonic and corresponds to a wavelength equal to the separation between the two parallel plates of 10 mm, while the subsequent peak at 35,580 Hz corresponds to one of the acoustics modes of the resonator. Although employing 4 elements per wavelength appears inadequate to capture the acoustic response, it becomes evident that utilizing 6 elements per wavelength with quadratic Lagrange elements proves sufficient for capturing the acoustic response while achieving a considerable reduction of the computational time from 35 hrs and 10 min for 8 elm/λ to 8 hrs and 3 min for 6 elm/λ (see Table 2).

Table 2: Numerical details of conducted simulations using COMSOL Multiphysics® for the simplified geometry of the FT wind sensor. BC=Boundary Condition; DB=Distance to Boundaries; DoF=Degree of Freedom. The direct solver MUMPS is used here.

ID	No Sym Sym	DB	elm/λ	DoF	BC	CPU(s)
01	No Sym	3 λ	4	885 k	PML	4827
02	No Sym	3 λ	6	2308 k	PML	30782
03	No Sym	3 λ	8	4815 k	PML	126624
04	Sym	3 λ	6	1178 k	PML	9877
05	Sym	2 λ	6	803 k	PML	4713
06	Sym	1 λ	6	489 k	PML	1966
07	Sym	0.5 λ	6	361 k	PML	1148
08	Sym	3 λ	6	533 k	IMP	1775
09	Sym	2 λ	6	355 k	IMP	981
10	Sym	1 λ	6	208 k	IMP	449
11	Sym	0.5 λ	6	149 k	IMP	281

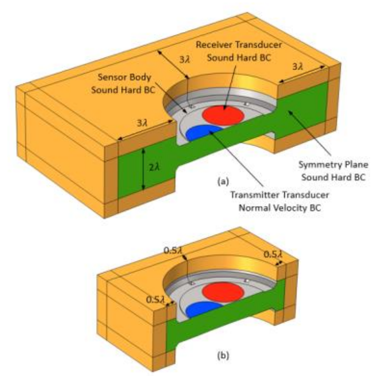

Figure 4: Details of (a) the extended domain and (b) reduced computational domain with a distance of 3λ and 0.5λ to PML.

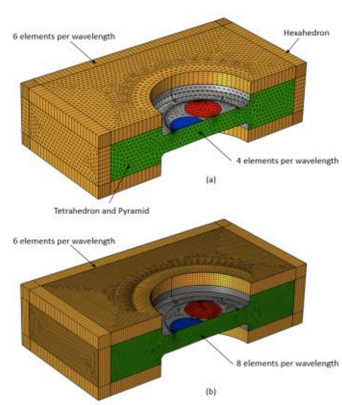

Figure 5: Details of the surface and volume mesh with a PML boundary condition using (a) 4 elm/λ and (b) 8 elm/λ.

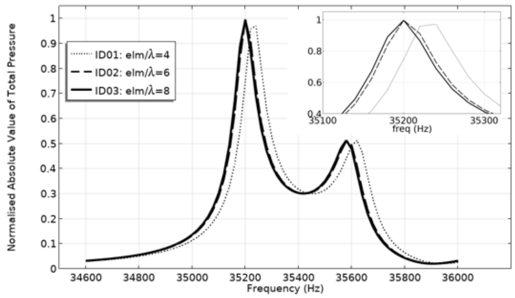

Figure 6: Effect of mesh density study on acoustic response with a PML boundary condition.

The effect of a symmetry plane on the acoustics response when using 6 elements per wavelength for a computational domain with a distance to the boundary equal to 3 λ (Figure 4 (a)) is shown in Figure 7 when comparing ID2 and ID4. No differences in the acoustic response are evident even though a significant reduction of the degree of freedom is achieved. Similarly, the influence of the computational domain's size is evaluated on the same graph by decreasing the distance from its boundary from 3 λ (ID4) to 0.5 λ (ID7), while keeping all other variables constant. No changes in the predictions of the first and second peaks are observed.

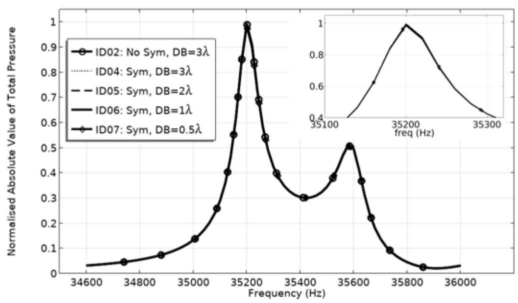

Figure 7: Effect of symmetry plane (ID02 vs ID04) and effect of computational domain size (ID04 to ID07) on acoustic response with a PML boundary condition.

The last test group evaluated here is the effect of replacing the PML with an impedance boundary condition (ID08-ID11 in Table 2) whereas reducing the computational domain from 3 λ to 0.5 λ and maintaining the size number of elements per wavelength of 6 (see Figure 8). Despite achieving a significant reduction in CPU usage (281s for ID11), no substantial variations were identified in the prediction of the first and second peaks' frequency when reducing the domain size. Similar results were obtained with PML boundary conditions.

The acoustics quality factor Q, associated with the initial peak, could serve as a performance metric of the numerical simulations, providing a quantitative assessment. The most refined mesh with no symmetric plane applied, and featuring the largest computational domain yields a value of 469 for the acoustics quality factor (ID03). The comparison with ID04 (see Table 2) led to a 1.23% reduction in Q-factor (see Figure 9). The effectiveness of the PML boundary condition in modelling the non-reflecting infinite domain is manifested by comparing ID04 (BC=3 λ) with ID07 (BC=0.5 λ) through Q-value. A mere 1.22% decrease is observed in Q-value whereas a 760% reduction on the CPU is achieved. A similar trend is observed when employing the impedance boundary condition with a reduction of 3.8% when compared ID08 (BC=3 λ) with ID11 (BC=0.5 λ) with a reduction of 531% on CPU.

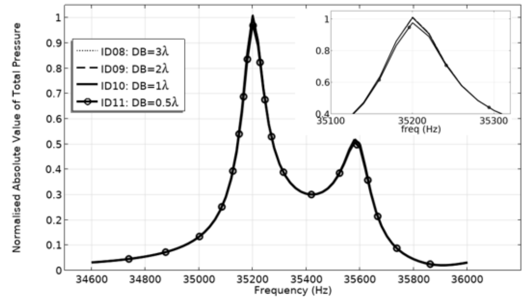

Figure 8: Effect of computational domain size on acoustic response with an impedance boundary condition.

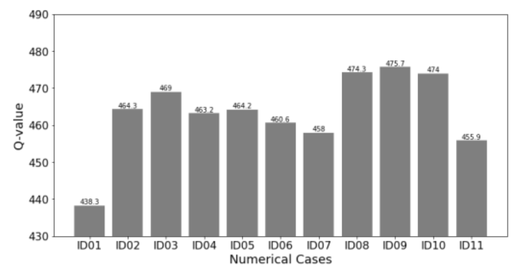

Figure 9: Q-value corresponding to the first peak for cases performed with COMSOL Multiphysics®.

The reason behind the minimal effect of the distance to the boundary either with PML or impedance boundary conditions on the acoustics signal and Q-value could be explained in Figure 10. It shows the total value of pressure at (a) the first peak frequency of 35,200 Hz and (b) the second peak frequency of 35,580 Hz for case ID4. As observed, the resonator effectively confines the acoustic field, minimizing the influence of the computational domain size on the acoustic response.

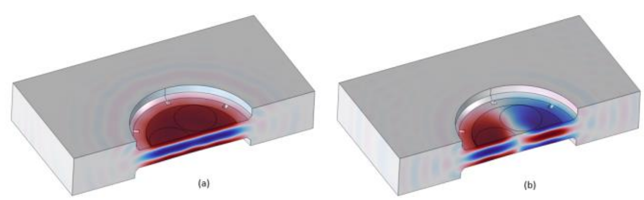

Figure 10: Total value of pressure at (a) 35,200 Hz and (b) 35,580 Hz for the case ID4 (see Table 2).

4.2.2. Results of NGSolve Acoustic Software

Considering the small impact of the treatment of the boundary condition on the acoustics field, the NGSolve acoustic software is evaluated with the use of the impedance boundary condition due to its ability to significantly reduce the CPU when compared with PML. Table 3 lists the numerical details of the simulations conducted with NGSolve with the direct solver Sparse Cholesky. This study involves the evaluation of two test groups. The first group focuses on the sensitivity of the solution to the mesh density (ID12-ID15) with a fixed computational domain size (BC=3 λ). After selecting the appropriate mesh, the second group (ID16-ID18) focused on the impact of the distance to the boundary condition on the acoustic field. It is noted that to accurately capture the frequencies of the first and second peaks and the Q-value, a minimum of 10 points per wavelength is required when using NGSolve with second-order Lagrange discretization schemes (see Figure 11 and Table 3). The impact of the distance to the boundary conditions is also reported in Table 3 through Q-value, and a 2.43% decrease is observed when comparing ID14 with ID18 whereas a reduction of 1014% on CPU is achieved.

Table 3: Numerical details of conducted simulations using NGSolve for the simplified geometry of the FT wind sensor. The direct solver Sparse Cholesky is used here.

ID	No Sym Sym	DB	elm/λ	DoF	BC	CPU(s)	Q-value
12	Sym	3 λ	6	164 k	IMP	1627	484.3
13	Sym	3 λ	8	367 k	IMP	8017	449.4
14	Sym	3 λ	10	696 k	IMP	33125	481.7
15	Sym	3 λ	12	1175 k	IMP	96110	476.7
16	Sym	2 λ	10	466 k	IMP	14720	482.3
17	Sym	1 λ	10	280 k	IMP	6373	480.9
18	Sym	0.5 λ	10	203 k	IMP	2971	465.1

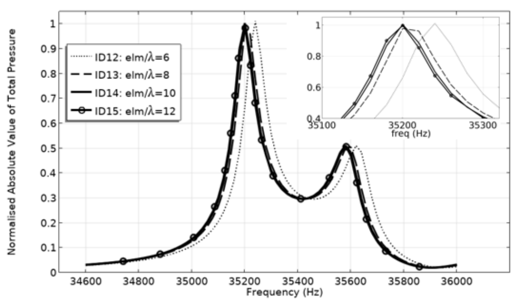

Figure 11: Effect of mesh density study on acoustic response with an impedance boundary condition.

Lastly, a comparison between the numerical solutions obtained with both acoustic software using the same computational domain size (BC=1 λ) is shown in Figure 12. Both curves are nearly indistinguishable with a difference in Q-factor of less than 1.5%. While COMSOL® simulations require 2.15 s per 1000 DoF when utilizing the direct solver MUMPS, NGSolve necessitates 22.76 s per 1000 DoF when employing the direct solver Sparse Cholesky on the same Desktop PC.

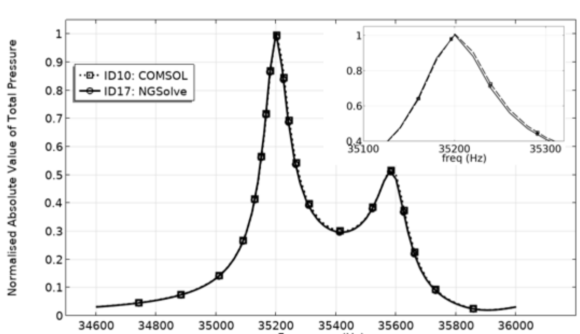

Figure 12: Numerical comparison between both acoustic software using the same computational domain size (BC=1 λ) of a simplified geometry of FT wind sensor.

5. CONCLUSIONS

The commercial acoustic software COMSOL Multiphysics® and the open-source finite element library NGSolve are compared in this study using a canonical 3D acoustic scattering problem at first, and a simplified geometry of a FT wind sensor. In the context of the scattering problem, to reduce the L^2 −errors within (10^{-1}), the use of at least eight elements per wavelength with second-order Lagrange approximation would be required for both software.

The acoustics field of the simplified FT wind sensor is not affected by using a symmetry condition. When using COMSOL®, simulations with PML and impedance boundary conditions require 6 elm/λ to capture the frequency of the first and second peaks. The effect of reducing the computational domain has a 1.22% and 3.8% decrease in Q-value for both boundary conditions, whereas a 760% and 531% reduction in the CPU are achieved. NGSolve requires a 10 elm/λ to accurately capture the main resonant frequency, and when compared to COMSOL®, a similar acoustics field is obtained. For the direct solvers study here, COMSOL® simulations show a CPU time that is one order of magnitude lower when compared with NGSolve. Further studies are needed to quantify how various direct and iterative solvers impact the CPU and memory loads.

6. REFERENCE

[1] FT Technologies. https://fttechnologies.com/. (Last Accessed: August 14, 2023).
[2] G. Quixley and A. Jimenez-Garcia, “Aerodynamic Analysis of FT Ultrasonic Wind Sensor Using Computational Fluid Dynamics”, 17th OpenFOAM Workshop, Cambridge, July, 2022.
[3] A. Noureddine, and F. Sgard. *Finite Element and Boundary Methods in Structural Acoustics and Vibration*. CRC Press, 2015.
[4] COMSOL Multiphysics® v. 6.1. www.comsol.com. COMSOL AB, Stockholm, Sweden. (Last Accessed: August 14, 2023).
[5] Joachim Schöberl, C++ 11 Implementation of Finite Elements in NGSolve. Tech. Rep. ASC-2014-30, Institute for Analysis and Scientific Computing, 2014.
[6] P. M. Morse, *Vibration and Sound*. Vol. 2. Acoustical Society of America, and American Institute of Physics. New York: McGraw-Hill, 1948.
[7] Acoustics Module User's Guide, pp. 63-153. COMSOL Multiphysics® v. 6.1. COMSOL AB, Stockholm, Sweden. 2022.
[8] Gmsh website. https://gmsh.info/. (Las Accessed: August 23, 2023).
[9] Lawrence E Kinsler, Austin R Frey, Alan B Coppens, and James V Sanders, *Fundamentals of Acoustics*, John Wiley & Sons, 2000.
[10] A. Sommerfeld. *Partial Differential Equations in Physics*. Academic press, 1949.
[11] ANSI Standard S1-26:1995, "Calculation of the Absorption of Sound by the Atmosphere" (ISO 9613-1:1996).
[12] S. Kapartis "Anemometer employing standing wave normal to fluid flow and travelling wave normal to standing wave." U.S. Patent No. 5,877,416. 2 Mar. 1999
[13] F. Ihlenburg and I. Babuška. “Finite Element Solution of the Helmholtz Equation with High Wave Number Part I: The h-version of the FEM,” *Computers & Mathematics with Applications*, vol. 30, no. 9, pp. 9–37, 1995.
[14] P. M Morse, H. Feshbach, and E. L. Hill. “Methods of Theoretical Physics,” *American Journal of Physics*, vol. 22, no. 6, pp. 410–413, 1954.